initiated the development of advanced electronic telephone line switching exchanges. From 1965 to 1973, he supervised a number of projects on data transmission, PCM, speech processing, and advanced line switching as Manager of Technology. He was appointed an IBM Fellow in 1975, and has published over 30 papers and filed more than 50 patents on data transmission and digital signal processing.

Some Windows with Very Good Sidelobe Behavior

ALBERT H. NUTTALL

Abstract—**Some of the windows presented by Harris [1] are not correct in terms of their reported peak sidelobes and optimal behavior. We present corrected plots of Harris' windows and also derive additional windows with very good sidelobes and optimal behavior under several different constraints. The temporal weightings are characterized as a sum of weighted cosines over a finite duration. The plots enable the reader to select a window to suit his requirements, in terms of bias due to nearby sidelobes and bias due to distant sidelobes.**

Introduction

THE use of temporal weightings for spectral analysis, with good sidelobe behavior and small bias, is well established and documented in Harris [1]. However, some of the plots of the spectral windows are not correct and do not have the optimal sidelobe levels claimed. We will present the corrected plots and some additional windows with optimal properties.

The temporal weightings considered will be continuous functions of time (except possibly at $t = \pm L/2$) and duration L, i.e.,

$$w(t) = 0 \quad \text{for} \quad |t| > L/2. \tag{1}$$

The Fourier transform of the temporal weighting is the spectral window

$$W(f) = \int_{-L/2}^{L/2} dt\, w(t) \exp(-i2\pi ft) \tag{2}$$

and is a continuous function of frequency, defined for all f. Notice the notational convention adopted here: a weighting is applied multiplicatively in one domain, and its Fourier transform (called a window) occurs as a convolution in the other domain.

All the window results presented here are obtained by exact analytical evaluation of (2) and are valid for all values of f. However, window (2) can be approximately evaluated at any f, by means of some numerical integration rule (such as trapezoidal), by choosing increment $\Delta = L/M$, where M is a large integer. These latter results are not adequate for $|f| > 0.5/\Delta$, because the approximation yielded by this numerical integration procedure has period $1/\Delta$ in f. Furthermore, if we limit the frequencies f, at which this numerical evaluation is conducted, to the values $n/(N\Delta)$ (for n and N integer), the results can be realized as an N-point discrete Fourier transform (DFT). Since the frequency spacing at which these values occur is $(N\Delta)^{-1}$ and the width of the spectral window (2) is of the order $1/L = (M\Delta)^{-1}$, we would also require $N > M$ if we desire to observe fairly closely the changes in the window (2) by means of an N-point DFT. There is no fundamental restriction on the relative sizes of M and N; however, M must be large in order to obtain an accurate approximation to (2).

Manuscript received July 8, 1980; revised August 5, 1980.

The author is with New London Laboratory, Naval Underwater Systems Center, New London, CT 06320.

General Weighting Considerations

The temporal weightings of interest here are of the form

$$w(t) = \frac{1}{L} \sum_{k=0}^{K} a_k \cos(2\pi kt/L) \quad \text{for} \quad |t| \leq L/2 \tag{3}$$

where $\{a_k\}_0^K$ are real constants. The weighting is symmetric about $t = 0$ and possesses all orders of derivatives for $|t| < L/2$; however, discontinuities in $w(t)$, defined by (1) and (3), or in its derivatives, occur at $t = \pm L/2$. These discontinuities dictate the asymptotic behavior for large $|f|$ of $W(f)$ in (2). Without loss of generality, the weighting is normalized according to

$$\sum_{k=0}^{K} a_k = 1; \quad w(0) = \frac{1}{L} \sum_{k=0}^{K} a_k = \frac{1}{L}. \tag{4}$$

Observe from (3) that

$$w\left(\pm \frac{L}{2}\right) = \lim_{|t| \to L/2-} w(t) = \frac{1}{L} \sum_{k=0}^{K} (-1)^k a_k, \tag{5}$$

which may or may not be equal to zero. If (5) is not zero, then weighting $w(t)$ is discontinuous at $t = \pm L/2$, and window $W(f)$ will decay only as $1/f$ for large f.

However, if (5) is zero, then $w(t)$ is continuous for all t.

Also, $w'(t)$ is continuous for all t since we always have

$$w'(t) = -\frac{2\pi}{L^2} \sum_{k=0}^{K} k a_k \sin(2\pi kt/L) \quad \text{for } |t| < L/2 \tag{6}$$

and

$$\lim_{|t| \to L/2-} w'(t) = 0; \quad w'(t) = 0 \quad \text{for } |t| > L/2. \tag{7}$$

The last property follows from (1). Thus, when weighting values $w(\pm L/2)$ in (5) are zero, $w(t)$ and $w'(t)$ are both continuous for all t.

However, $w''(t)$ may then not be continuous at $t = \pm L/2$. We have from (6),

$$w''(t) = -\frac{4\pi^2}{L^3} \sum_{k=0}^{K} k^2 a_k \cos(2\pi kt/L) \quad \text{for } |t| < L/2 \tag{8}$$

and

$$\lim_{|t| \to L/2-} w''(t) = -\frac{4\pi^2}{L^3} \sum_{k=0}^{K} (-1)^k k^2 a_k, \tag{9}$$

which may or may not be zero. If (9) is not zero, then $w''(t)$ is discontinuous at $t = \pm L/2$, and $W(f)$ will decay as $1/f^3$ for large f.

Conversely, if (9) is zero, then $w''(t)$ is continuous for all t, and it follows (similarly to above) that $w'''(t)$ is continuous for all t. Then $W(f)$ decays at least as fast as $1/f^5$ for large f. We will have occasion to use these relations later.

The spectral window corresponding to $w(t)$ in (1) and (3) is given by (2) as the closed form expression

$$W(f) = \frac{Lf}{\pi} \sin(\pi Lf) \sum_{k=0}^{K} \frac{(-1)^k a_k}{L^2 f^2 - k^2} \quad \text{for all } f;$$

$$W(n/L) = \begin{cases} a_0, & n = 0 \\ \frac{1}{2} a_{|n|}, & n \neq 0 \end{cases}. \tag{10a}$$

If we expand $(L^2 f^2 - k^2)^{-1}$ in a power series in $(k/Lf)^2$, we obtain

$$W(f) = \frac{\sin(\pi Lf)}{\pi Lf} \sum_{m=0}^{\infty} \frac{1}{(Lf)^{2m}} \sum_{k=0}^{K} (-1)^k k^{2m} a_k$$

$$\text{for } |Lf| > K. \tag{10b}$$

Thus, the quantities (5) and (9) considered above are simply the $m = 0$ and $m = 1$ coefficients of this expansion; the asymptotic behavior of (10b) depends on the first nonzero term in the m-series, and will be plotted in the following figures as a dotted line.

Discrete Fourier Series

When continuous temporal weighting is used in digital processing, it is sampled and often transformed into the frequency domain, where its effect can be included as a convolution of its discrete Fourier series with the data DFT. To evaluate this discrete Fourier series, we begin by delaying the temporal weight to the interval $(0, L)$:

$$w_D(t) \equiv w\left(t - \frac{L}{2}\right) = \frac{1}{L} \sum_{k=0}^{K} (-1)^k a_k \cos(2\pi kt/L)$$

$$= \frac{1}{L} \sum_{k=-K}^{K} (-1)^k \epsilon_k a_{|k|} \exp(i2\pi kt/L)$$

$$\text{for } 0 \leqslant t \leqslant L \tag{11}$$

where

$$\epsilon_k = \begin{cases} 1, & k = 0 \\ \frac{1}{2}, & k \neq 0 \end{cases}. \tag{12}$$

Let the sampling interval on weighting $w_D(t)$ be

$$\Delta = L/M \tag{13}$$

where M is even; then samples (temporal weights)

$$w_D(m\Delta) = \frac{1}{L} \sum_{k=-K}^{K} (-1)^k \epsilon_k a_{|k|} \exp(i2\pi km/M)$$

$$\text{for } 0 \leqslant m \leqslant M. \tag{14}$$

Then for $M > 2K$, the discrete Fourier series is given by the M-point DFT [2, ch. 3][1]

$$\sum_{m=0}^{M-1} \Delta w_D(m\Delta) \exp(-i2\pi mn/M) = (-1)^n \epsilon_n a_{|n|}$$

$$\text{for } |n| \leqslant M/2. \tag{15a}$$

Thus, the effects of temporal weighting (14) can be incorporated in a digital processing application as a frequency convolution of the data DFT with the sequence

$$\cdots, 0, 0, (-1)^K \tfrac{1}{2} a_K, \cdots, -\tfrac{1}{2} a_1, a_0, -\tfrac{1}{2} a_1, \cdots,$$
$$(-1)^K \tfrac{1}{2} a_K, 0, 0, \cdots. \tag{15b}$$

This is one of the main reasons for employing weightings of the form (14) in digital processing applications; namely, the effects of temporal weighting are easily included by means of convolution in the discrete frequency domain with a short sequence of length $2K + 1$.

The effect of sampling continuous weighting $w(t)$ at increment Δ, in so far as the effective window is concerned, is as follows. The effective window is

$$W_e(f) = \int_{-\infty}^{+\infty} dt\, \Delta\delta_\Delta(t)\, w(t) \exp(-i2\pi ft)$$

$$= \delta_{1/\Delta}(f) \circledast W(f) = \sum_{n=-\infty}^{\infty} W\left(f - \frac{n}{\Delta}\right) \tag{16}$$

where $\delta_a(x)$ is an infinite unit-area impulse train in x at spacing a. Thus, there are periodic replications in $W_e(f)$ at multiples of $1/\Delta$; the aliasing at $f = \pm 0.5/\Delta$ is obvious. All the following results correspond to $\Delta = 0$, i.e., continuous weightings; thus, there is no aliasing.

[1] This consideration is different from that mentioned under (2), where we were interested in approximately evaluating window $W(f)$ in (2) by means of a DFT.

HARRIS' WINDOWS

The first weighting to be considered is Hanning, for which there are only two nonzero coefficients in (3):

$$a_0 = 0.5, \quad a_1 = 0.5 \qquad W(f) = \frac{\sin(\pi L f)}{2\pi L f(1 - L^2 f^2)}. \tag{17}$$

Its power response in dB is plotted versus Lf in Fig. 1, normalized to the peak response at $f = 0$; that is

$$\text{dB} \equiv 10 \log |W(f)/W(0)|^2 \tag{18}$$

is plotted.[2] The largest sidelobe is -31.47 dB. Since (5) is zero for the weights in (17), but (9) is not, the Hanning window has an asymptotic decay of 18 dB/octave; this decay is the first nonzero term in (10b).

The second weighting is Blackman [1, eq. 32]:

$$a_0 = 0.42, \quad a_1 = 0.50, \quad a_2 = 0.08. \tag{19}$$

The window is depicted in Fig. 2. Again, (5) is zero, but (9) is not; thus the asymptotic decay is 18 dB/octave. The largest sidelobe is -58.11 dB.

The "exact" Blackman weights are [1, p. 63]

$$a_0 = 7938/18608, \quad a_1 = 9240/18608, \quad a_2 = 1430/18608. \tag{20}$$

Now (5) is not zero; therefore, the window decays at only 6 dB/octave as shown in Fig. 3. However, the largest sidelobe is -68.24 dB, not -51 dB as cited in [1, Fig. 23]. Also, the sidelobes in Fig. 3 are about 6 dB lower than those reported in [1, Fig. 23].

The following four windows are listed in the table in [1, p. 65]. The "minimum" 3-term weights are

$$a_0 = 0.42323, \quad a_1 = 0.49755, \quad a_2 = 0.07922. \tag{21}$$

Since (5) is not zero, the window decay is only 6 dB/octave, as shown in Fig. 4. The maximum sidelobe is -70.83 dB, not -67 dB as reported in [1, Fig. 24 and p. 64].

The 3-term weights are

$$a_0 = 0.44959, \quad a_1 = 0.49364, \quad a_2 = 0.05677. \tag{22}$$

The corresponding window is given in Fig. 5 and has a maximum sidelobe of -62.05 dB, rather than the -61 dB reported in [1, p. 65]. Since (5) is not zero, the decay is only at 6 dB/octave, as indicated by the dotted line.

The "minimum" 4-term weights are[3]

$$a_0 = 0.35875, \quad a_1 = 0.48829, \quad a_2 = 0.14128, \quad a_3 = 0.01168. \tag{23}$$

[2]When the weighting is applied instead in the lag domain, as for Blackman-Tukey spectral analysis, rather than in the time domain as presumed here, the window appears linearly rather than as its square. In this case, the square must be removed from the definition in (18), and all the plots require that the dB numbers on the ordinate be halved. For example, the peak Hanning sidelobe is then -15.73 dB.

[3]These are not the weights actually listed in [1, p. 65]. However, the values listed there do not add up to 1; accordingly, we have modified them according to the comment under (34), and made them sum to 1 (with the lowest sidelobe possible by modifying just one of the last digits).

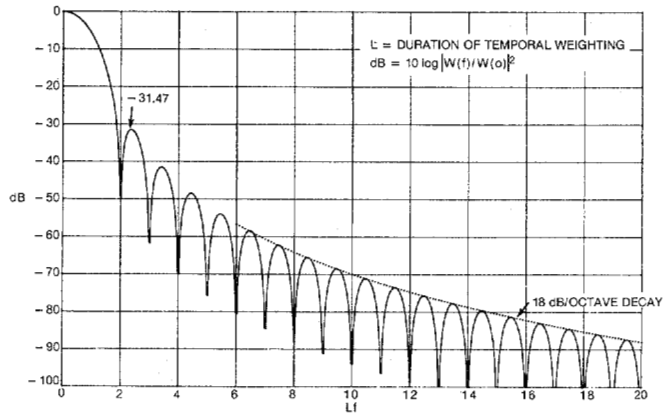

Fig. 1. Hanning window for $a_0 = 0.5, a_1 = 0.5$.

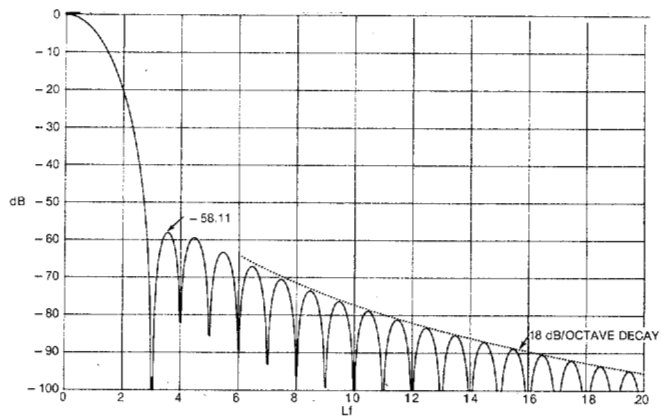

Fig. 2. Blackman window for $a_0 = 0.42, a_1 = 0.5, a_2 = 0.08$.

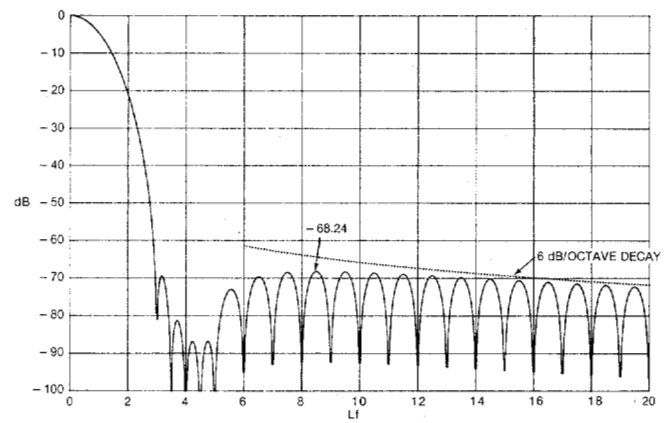

Fig. 3. Exact Blackman window for $a_0 = 7938/18608$, $a_1 = 9240/18608$, $a_2 = 1430/18608$.

Although (5) is not zero, it is nearly so. Therefore, the initial decay of the window is greater than 6 dB/octave; however, it must eventually decay only as 6 dB/octave. The maximum sidelobe of the window is indicated in Fig. 6; it is -92 dB, as reported in [1].

The 4-term weights are

$$a_0 = 0.40217, \quad a_1 = 0.49703, \quad a_2 = 0.09892, \quad a_3 = 0.00188. \tag{24}$$

The asymptotic decay is only 6 dB/octave, as shown in Fig. 7, and the largest sidelobe is -74.39 dB, as claimed in [1, p. 65].

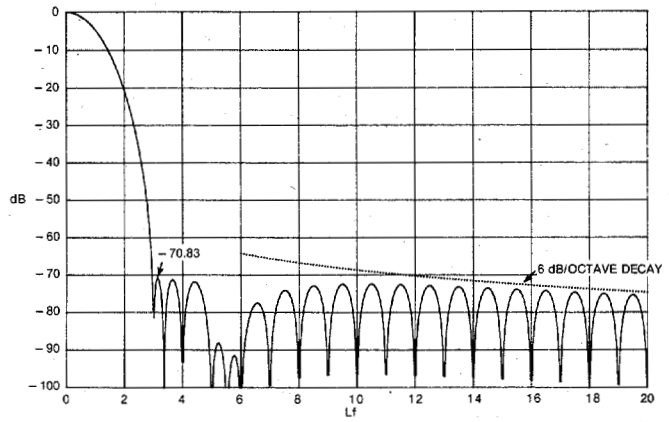

Fig. 4. "Minimum" 3-term window for $a_0 = 0.42323$, $a_1 = 0.49755$, $a_2 = 0.07922$.

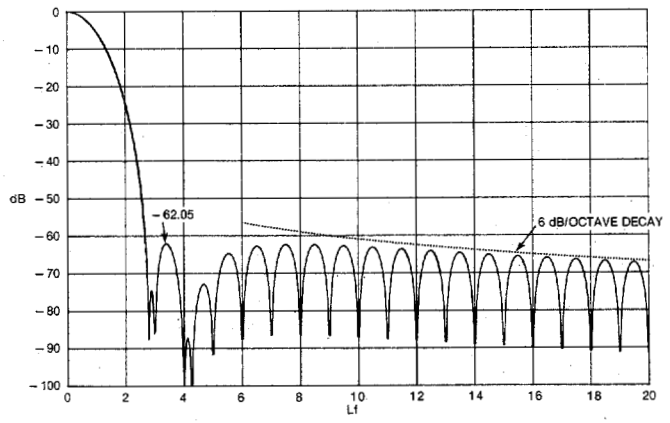

Fig. 5. 3-Term window for $a_0 = 0.44959$, $a_1 = 0.49364$, $a_2 = 0.05677$.

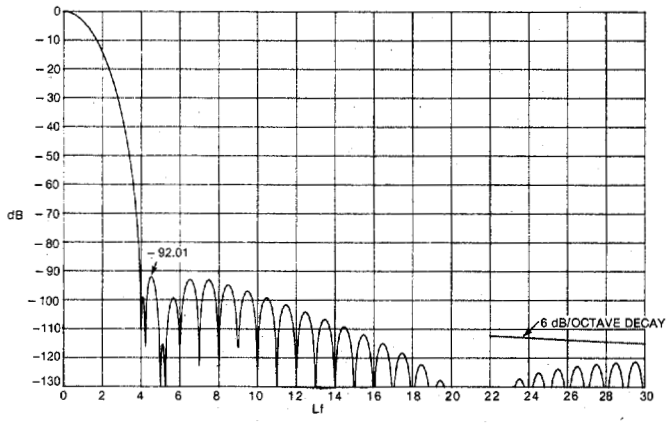

Fig. 6. "Minimum" 4-term window for $a_0 = 0.35875$, $a_1 = 0.48829$, $a_2 = 0.14128$, $a_3 = 0.01168$.

Rapidly Decaying Windows with Minimal Sidelobes

It was observed earlier that the window $W(f)$ decays fairly rapidly for large f if (5) is zero, and very rapidly if (9) is zero. Such windows will lead to spectral estimates that are immune to strong interferences at frequencies removed from those of interest. In this section, we will consider this class of windows in terms of the peak sidelobe and asymptotic decay; the mainlobe width of each window is not discussed, but is easily determined from the plots. Discontinuous weightings will be taken up later.

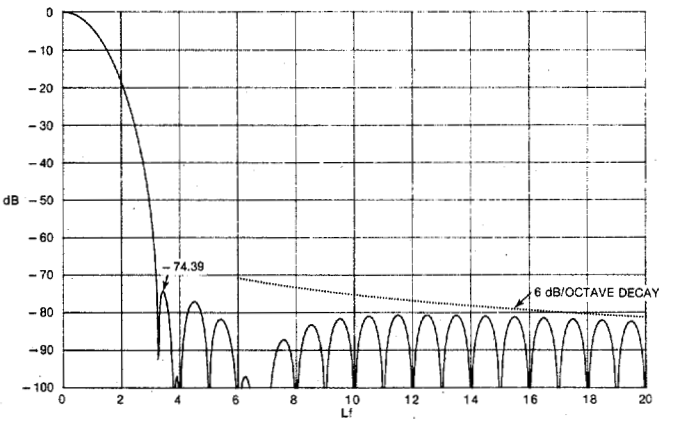

Fig. 7. 4-Term window for $a_0 = 0.40217$, $a_1 = 0.49703$, $a_2 = 0.09892$, $a_3 = 0.00188$.

If only two coefficients in weighting (3) are nonzero, satisfaction of (4), and setting (5) equal to zero, yield

$$a_0 + a_1 = 1, \quad a_0 - a_1 = 0. \tag{25}$$

The Hanning window satisfies these requirements and is plotted in Fig. 1. Convolution sequence (15b) is simply $-1/4$, $1/2$, $-1/4$.

Moving on to three nonzero coefficients in (3), if we satisfy (4), and set (5) and (9) equal to zero, we find

$$a_0 = 3/8, \quad a_1 = 4/8, \quad a_2 = 1/8. \tag{26}$$

The weighting is

$$w(t) = \frac{1}{L} \cos^4 (\pi t/L) \quad \text{for} \quad |t| \leqslant L/2. \tag{27}$$

From (15b), the discrete Fourier series for convolution is

$$\frac{1, -4, 6, -4, 1}{16} \tag{28}$$

which are simply the binomial coefficients. As noted under (9), since the third derivative of $w(t)$ is continuous at $t = \pm L/2$, the window decays at a 30 dB/octave rate. The plot in Fig. 8 indicates that the largest sidelobe is -46.74 dB.

Instead of forcing (9) equal to zero, we can use the one degree of freedom left, after (4) is satisfied and (5) is set equal to zero, to minimize the maximum sidelobes. The optimal weights are found to be

$$a_0 = 0.40897, \quad a_1 = 0.5, \quad a_2 = 0.09103. \tag{29}$$

The corresponding window is presented in Fig. 9. The asymptotic decay is 18 dB/octave, and the two equal sidelobes are of size -64.19 dB. This is 6.1 dB better than the -58.1 dB sidelobe of the Blackman window, yet the asymptotic decays are equal. Although the maximum sidelobe of the "minimum" 3-term window in Fig. 4 is 6.6 dB better, that decay is only 6 dB/octave rather than the 18 dB/octave decay here.

When we consider four nonzero coefficients in (3), we have several alternatives. If we satisfy (4), set (5) and (9) both equal to zero, and also set the fourth derivative of $w(t)$ equal to zero at $t = \pm L/2$, we have four equations in four unknowns, with solution

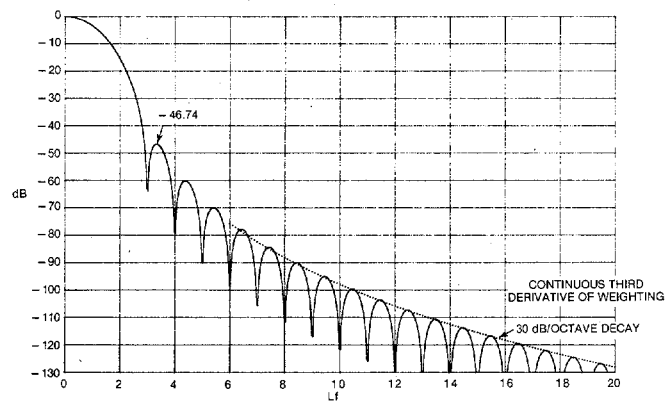

Fig. 8. Window for $a_0 = 0.375, a_1 = 0.5, a_2 = 0.125$.

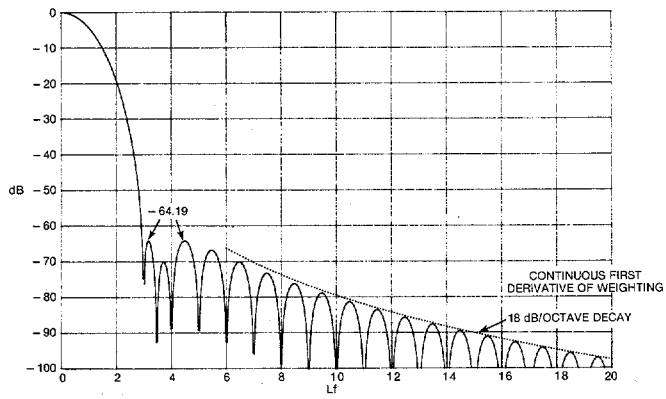

Fig. 9. Window for $a_0 = 0.40897, a_1 = 0.5, a_2 = 0.09103$.

$$a_0, a_1, a_2, a_3 = \frac{10, 15, 6, 1}{32}. \tag{30}$$

The weighting is

$$w(t) = \frac{1}{L} \cos^6 (\pi t/L) \quad \text{for} \quad |t| \leqslant \frac{L}{2} \tag{31}$$

and from (15b), the discrete Fourier series for convolution is

$$\frac{-1, 6, -15, 20, -15, 6, -1}{64} \tag{32}$$

which are again the binomial coefficients. The window decays at a very fast rate of 42 dB/octave, since the fifth derivative of $w(t)$ is continuous for all t. The plot in Fig. 10 shows the maximum sidelobe to be -60.95 dB.

If we satisfy (4), and set (5) and (9) both equal to zero, but use the remaining degree of freedom to minimize the maximum sidelobes, the optimal weights are determined to be

$$a_0 = 0.338946, \quad a_1 = 0.481973, \quad a_2 = 0.161054,$$
$$a_3 = 0.018027. \tag{33}$$

The window is given in Fig. 11 and has two equal sidelobes of -82.60 dB. The asymptotic decay is 30 dB/octave, since the third derivative of $w(t)$ is continuous for all t. Comparison with the "minimum" 4-term window in Fig. 6 reveals a difference of 9.4 dB in the maximum sidelobe; however, the decay of Fig. 11 is much faster at a 30 dB/octave rate. As far as the 4-term window in Fig. 7 is concerned, Fig. 11 has an 8.2 dB better maximum sidelobe and a much better decay, 30 dB/octave versus 6 dB/octave.

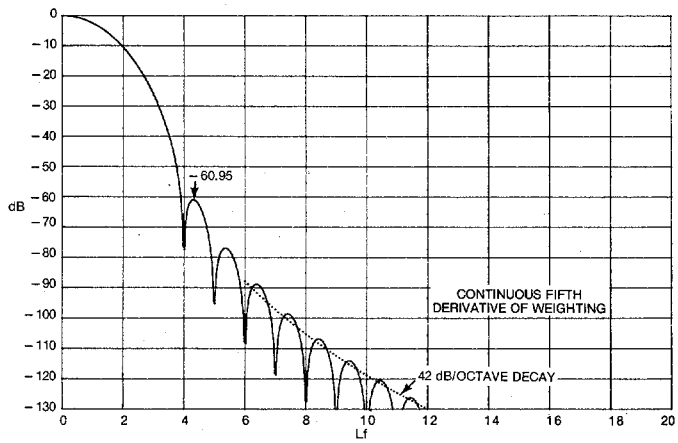

Fig. 10. Window for $a_0 = 10/32, a_1 = 15/32, a_2 = 6/32, a_3 = 1/32$.

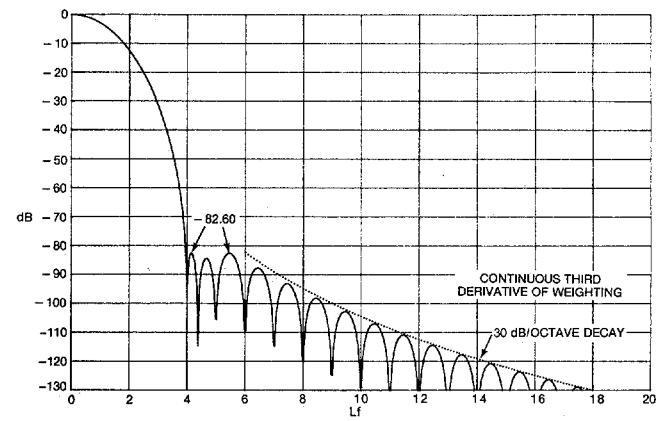

Fig. 11. Window for $a_0 = 0.338946$, $a_1 = 0.481973$, $a_2 = 0.161054$, $a_3 = 0.018027$.

Finally, if we satisfy (4), and set only (5) equal to zero, and use the remaining two degrees of freedom to minimize the maximum sidelobes, the optimal weights are found to be

$$a_0 = 0.355768, \quad a_1 = 0.487396, \quad a_2 = 0.144232,$$
$$a_3 = 0.012604. \tag{34}$$

The window is shown in Fig. 12 and has three equal sidelobes of -93.32 dB. Notice that this level is better than the purported "minimum" 4-term level of -92 dB claimed in [1, pp. 64-65]; and the asymptotic decay is 18 dB/octave, not 6 dB/octave. Furthermore, this level was achieved under the constraint of setting (5) equal to zero. If we were to eliminate this constraint of a continuous weighting function, a sidelobe level lower than -93.32 dB can be achieved. (This problem and the determination of the true minimum 3-term window (to replace Fig. 4) are undertaken in the next section.) Comparison with the 4-term window of Fig. 7 reveals an 18.9 dB peak-sidelobe improvement in Fig. 12 and a better decay of 18 dB/octave instead of 6 dB/octave.

Minimum Sidelobe Windows

If only two coefficients in weighting (3) are nonzero, and we disregard the continuity requirement (5), the one degree of

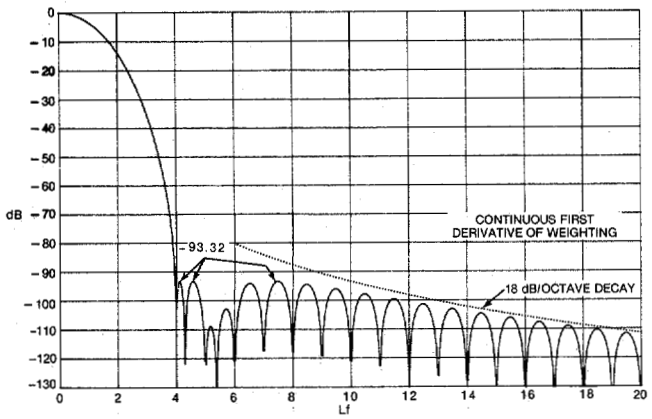

Fig. 12. Window for $a_0 = 0.355768$, $a_1 = 0.487396$, $a_2 = 0.144232$, $a_3 = 0.012604$.

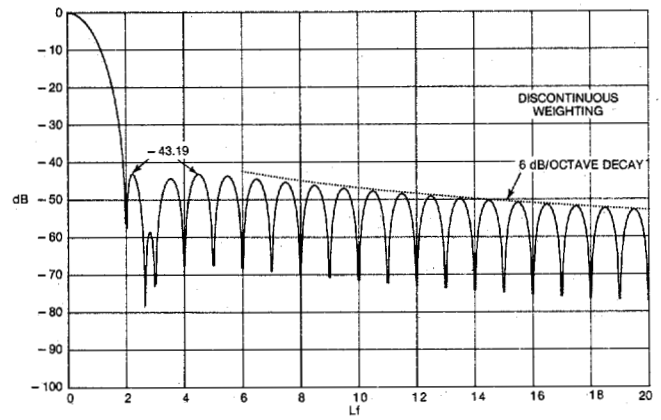

Fig. 13. Hamming window for $a_0 = 0.53836$, $a_1 = 0.46164$.

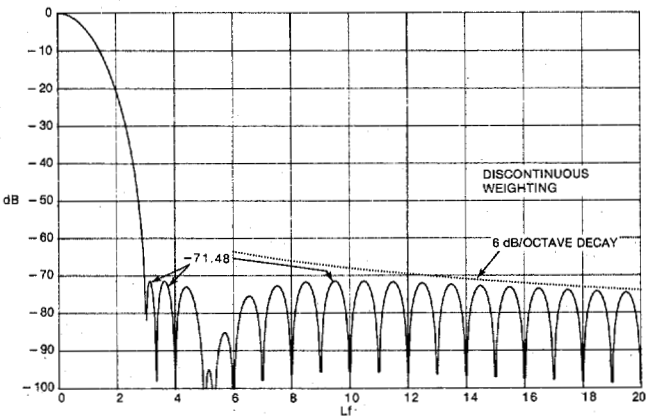

Fig. 14. Minimum 3-term window for $a_0 = 0.4243801$, $a_1 = 0.4973406$, $a_2 = 0.0782793$.

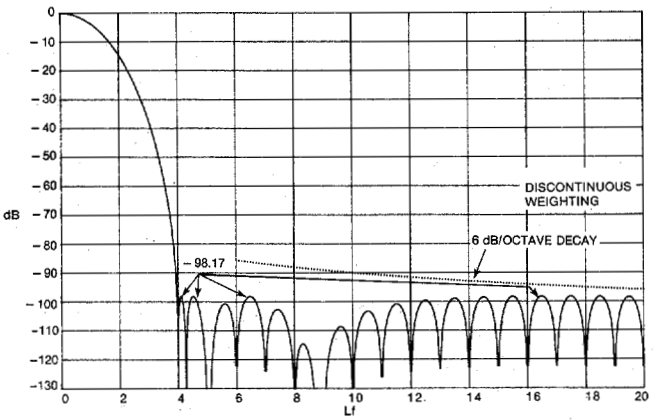

Fig. 15. Minimum 4-term window for $a_0 = 0.3635819$, $a_1 = 0.4891775$, $a_2 = 0.1365995$, $a_3 = 0.0106411$.

freedom left, after normalization (4) is satisfied, can be used to minimize the maximum sidelobes. The result is the familiar Hamming window, plotted in Fig. 13, with coefficients

$$a_0 = 0.53836, \quad a_1 = 0.46164. \tag{35}$$

The two equal peak-sidelobes are -43.19 dB, and the asymptotic decay is only 6 dB/octave, as dictated by (10b) when (5) is not zero.

For three nonzero coefficients in (3), satisfaction of (4) leaves two degrees of freedom. These can be used to realize the minimum 3-term window in Fig. 14, for which the optimal coefficients are

$$a_0 = 0.4243801, \quad a_1 = 0.4973406, \quad a_2 = 0.0782793. \tag{36}$$

There are three equal peak-sidelobes of -71.48 dB, which is 0.65 dB better than Fig. 4, with an asymptotic decay of 6 dB/octave for both.

When four coefficients are nonzero in (3), there are three degrees of freedom left after normalization (4). The minimum 4-term window results for coefficients

$$a_0 = 0.3635819, \quad a_1 = 0.4891775, \quad a_2 = 0.1365995,$$
$$a_3 = 0.0106411 \tag{37}$$

and is shown in Fig. 15. The four equal sidelobes are at level -98.17 dB, which is 6.16 dB better than Fig. 6, with an asymptotic decay of 6 dB/octave for both. This sidelobe level is 4.85 dB better than Fig. 12, but the decay in Fig. 12 is 18 dB/octave.

Comparison with Kaiser-Bessel and van der Maas Windows

The windows in Figs. 13-15 are very similar to the Kaiser-Bessel window. Specifically, the Kaiser-Bessel weighting and window are

$$w(t) = \frac{1}{L} I_0(B\sqrt{1 - (2t/L)^2}) \quad \text{for} \quad |t| < L/2,$$
$$W(f) = \frac{\sin(\sqrt{\pi^2 L^2 f^2 - B^2})}{\sqrt{\pi^2 L^2 f^2 - B^2}} \quad \text{for all } f, \tag{38}$$

respectively, where B is a parameter. If we choose B to make the first null of the Kaiser-Bessel window lie at the three alternatives of $Lf = 2, 3, 4$ (as in Figs. 13-15, respectively), we obtain the plots in Figs. 16-18. The corresponding mainlobe shapes are indistinguishable, and the asymptotic decays are all 6 dB/octave. The immediate sidelobes of the Kaiser-Bessel windows are several dB larger than the minimum results in Figs. 13-15, but the distant sidelobes of the Kaiser-Bessel windows are over 10 dB lower for the examples considered. Thus, a tradeoff exists between the peak sidelobe and the distant sidelobe level.

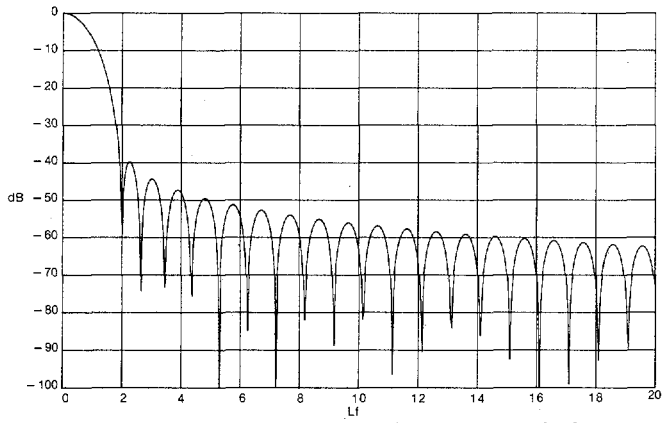

Fig. 16. Kaiser-Bessel window with first null at $Lf = 2$.

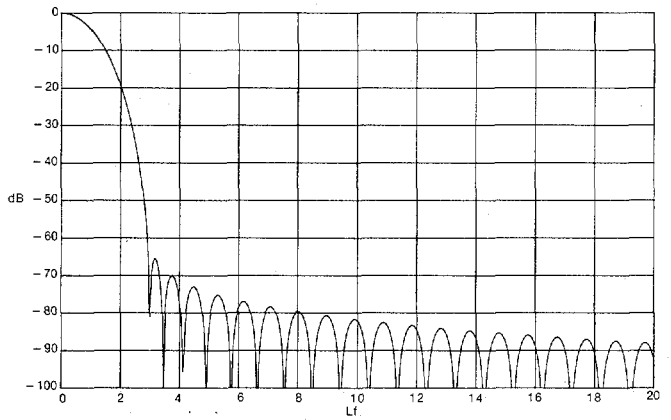

Fig. 17. Kaiser-Bessel window with first null at $Lf = 3$.

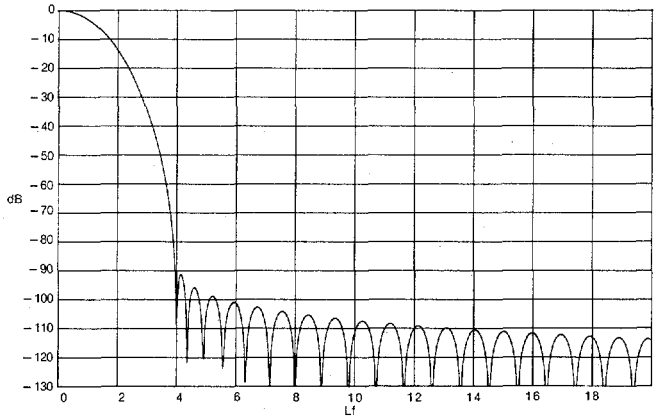

Fig. 18. Kaiser-Bessel window with first null at $Lf = 4$.

The windows here are also similar to the ideal impulsive van der Maas window given by

$$w(t) = \frac{B}{L}\,\frac{I_1(B\sqrt{1-(2t/L)^2})}{\sqrt{1-(2t/L)^2}} + \frac{1}{2}\,\delta\left(t-\frac{L}{2}\right) + \frac{1}{2}\,\delta\left(t+\frac{L}{2}\right) \quad \text{for } |t| \leq \frac{L}{2},$$

$$W(f) = \cos\left(\sqrt{(\pi Lf)^2 - B^2}\right) \quad \text{for all } f. \tag{39}$$

This window is characterized by having the narrowest possible mainlobe width for a specified sidelobe level, and vice versa. However, the window does not decay at all for large f. The peak to sidelobe voltage level is $SL \equiv \cosh(B)$, and the first null of the window occurs at

TABLE I
COMPARISON OF NULL LOCATION WITH VAN DER MAAS CASE

Figure Number	Null Location	van der Maas Null Location
9	3	2.62
11	4	3.29
12	4	3.67
13	2	1.87
14	3	2.88
15	4	3.85

TABLE II
WINDOW CHARACTERISTICS

Weighting	Peak Sidelobe (dB)	Asymptotic Decay (dB/octave)
1. Hanning	-31.47	18
2. Blackman	-58.11	18
3. Exact Blackman	-68.24	6
4. "Minimum" 3-Term	-70.83	6
5. 3-Term	-62.05	6
6. "Minimum" 4-Term	-92.01	6
7. 4-Term	-74.39	6
8. 3-Term with Continuous Third Derivative	-46.74	30
9. 3-Term with Continuous First Derivative	-64.19	18
10. 4-Term with Continuous Fifth Derivative	-60.95	42
11. 4-Term with Continuous Third Derivative	-82.60	30
12. 4-Term with Continuous First Derivative	-93.32	18
13. Hamming	-43.19	6
14. Minimum 3-Term	-71.48	6
15. Minimum 4-Term	-98.17	6
16. Kaiser-Bessel Window with First Null at $Lf = 2$	-39.79	6
17. Kaiser-Bessel Window with First Null at $Lf = 3$	-65.45	6
18. Kaiser-Bessel Window with First Null at $Lf = 4$	-91.22	6

$$Lf_0 = \left(\frac{1}{4} + \frac{B^2}{\pi^2}\right)^{1/2}. \tag{40}$$

Thus, the first null location can be expressed in terms of the sidelobe level SL according to

$$Lf_0 = \left(\frac{1}{4} + \left[\frac{\ln\left(SL + \sqrt{SL^2 - 1}\right)}{\pi}\right]^2\right)^{1/2}. \tag{41}$$

Table I shows this null location and the actual location for several of the windows presented earlier, when the peak sidelobes are equal; the agreement is close, especially for those windows with a 6 dB/octave decay, Figs. 13-15.

SUMMARY

When strong interference, either tonal or narrow band, occurs additively with a desired signal, its effect on frequencies removed from the interference band can be greatly reduced by using windows with low sidelobes and significant decay of the sidelobes. Thus, close-by interference rejection requires the immediate sidelobe region of the window to be small, while distant interference rejection requires a rapidly decaying sidelobe response. The type of windows considered here furnish several alternative choices, depending on the application of

interest, and range from -31 dB to -98 dB for the peak sidelobe, or 6 dB/octave to 42 dB/octave for the asymptotic decay. The weighting given by (3) is nonnegative for all the numerical coefficients listed here. A summary of the windows is presented in Table II. An application of these windows to a discrete Hilbert transform is given in [3].

References

[1] F. J. Harris, "On the use of windows for harmonic analysis with the discrete Fourier transform," *Proc. IEEE*, vol. 66, pp. 51-83, Jan. 1978.
[2] A. V. Oppenheim and R. W. Schafer, *Digital Signal Processing.* Englewood Cliffs, NJ: Prentice-Hall, 1975.
[3] A. H. Nuttall, "Some windows with very good sidelobe behavior; application to a discrete Hilbert transform," NUSC Tech. Rep. 6239, Apr. 9, 1980.

Albert H. Nuttall received the B.S., M.S., and Sc.D. degrees in electrical engineering from the Massachusetts Institute of Technology, Cambridge, in 1954, 1955, and 1958, respectively.

He was an Assistant Professor of Electrical Engineering at M.I.T. for one year. From 1957 to 1960 he was with Melpar, Inc. and from 1960 to 1968 was with Litton Industries. Since 1968 he has been with the Naval Underwater Systems Center, New London, CT. He is in the field of Statistical Communication Theory and serves as a Laboratory Consultant and is involved in applications of probability theory and statistics to underwater acoustics problems.

On the Application of a Fast Polynomial Transform and the Chinese Remainder Theorem to Compute a Two-Dimensional Convolution

T. K. TRUONG, IRVING S. REED, FELLOW, IEEE, RICHARD G. LIPES, MEMBER, IEEE, AND CHIALIN WU

Abstract—**In this paper, a fast algorithm is developed to compute two-dimensional convolutions of an array of $d_1 \times d_2$ complex number points where $d_2 = 2^m$ and $d_1 = 2^{m-r+1}$ for some $1 \leq r \leq m$. This new algorithm requires fewer multiplications and about the same number of additions as the conventional FFT method for computing the two-dimensional convolution. It also has the advantage that the operation of transposing the matrix of data can be avoided.**

Introduction

TWO-DIMENSIONAL convolutions of two sequences of complex number points can be applied to many areas, in particular to the synthetic aperture radar (SAR) [1], [2]. In SAR, a two-dimensional cross correlation of the new echo data of complex numbers with the response function of a point target is required to produce images. When the two-dimensional filter does not change rapidly with the range, one can divide the entire range of echo data into several subintervals. Within each subinterval one can use a constant filter function. This is accomplished usually by using the conventional fast Fourier transform (FFT). However, the FFT algorithm generally requires a large number of floating-point complex additions and multiplications. Also, the transpose of a matrix is usually required in the computation of such a two-dimensional convolution.

Recently, Rader [3] proposed that a number-theoretic transform (NTT) could be used to accomplish two-dimensional filtering. It was shown [4] that an improvement both in accuracy and speed of two-dimensional convolutions could be achieved by transforms over a finite field $GF(q)$ where q is a prime of the form $45 \times 2^{29} + 1$. However, to compute a two-dimensional convolution of two long sequences of an integer number of points, such a transform over a finite field did not allow for a wide variety of dynamic ranges.

More recently, Nussbaumer [5] first defined a type of polynomial transform over the fields of polynomial which could be used to efficiently compute two-dimensional convolutions. A principal advantage of this method over the above-mentioned techniques is that the need for computing the transpose of the matrix can be avoided. Furthermore, this new method offers a wider variety of dynamic ranges. It was shown [6]-[8] that the ideas of Nussbaumer can be generalized to a radix-2 polynomial transform analogous to the conventional radix-2 FFT. They make use of the Chinese remain-

Manuscript received December 3, 1979; revised June 4, 1980. This work was supported in part by NASA under Contract NAS7-100 and in part by the U.S. Air Force Office of Scientific Research under Grant AFOSR-80-0151.

T. K. Truong, R. G. Lipes, and C. Wu are with the Jet Propulsion Laboratory, Pasadena, CA 91103.

I. S. Reed is with the Department of Electrical Engineering, University of Southern California, Los Angeles, CA 90007.

0096-3518/81/0200-0091$00.75